ELSEVIER

Journal of Hazardous Materials 53 (1997) 57–74

JOURNAL OF HAZARDOUS MATERIALS

Surface chemical interaction of fibrous asbestos with biocells: An ESCA study

Sudipta Seal [a], Susan Krezoski [b], Tery L. Barr [a,*], David H. Petering [b], Peter H. Evans [c], Jacek Klinowski* [c]

[a] *Department of Materials and Laboratory for Surface Studies, University of Wisconsin-Milwaukee, Milwaukee, Wisconsin 53201, USA*

[b] *Department of Chemistry, University of Wisconsin-Milwaukee, Milwaukee, Wisconsin 53201, USA*

[c] *Department of Chemistry, University of Cambridge, Lensfield Road, Cambridge CB2 1EW, UK*

Received 13 March 1996; accepted 9 September 1996

Abstract

High-resolution X-ray Photoelectron Spectroscopy (XPS), also known as ESCA (Electron Spectroscopy for Chemical Analysis), has been used to monitor the surface chemistry of silicate minerals exposed to living cells. We have followed the chemical changes in the silicates induced by changes in elemental composition (reflected in the Si/Al and Si/Mg ratios) and structure. Changes in bond strength which occur in the process were monitored via the line shifts in the ESCA spectra. As it is likely that differences in surface chemistry affect the interactions of silicates with cellular systems, we have embarked on a systematic study of well-characterized silicates exposed to murine tumour Ehrlich cells under controlled conditions. ESCA identifies changes in the surface chemistry of asbestos caused by interactions with cells, while atomic absorption spectrometry (AAS) monitors silicate-induced changes in the cell iron content. There is a significant increase in iron concentration in the cells and in the Si/Mg ratio on the surface of asbestos after contact with the cells. The complex C(1s) and Si(2p) ESCA spectral features and the presence of trace elements in freeze-dried cell–asbestos mixtures indicate the presence of chemical interactions of asbestos with the cells. We believe that such studies may eventually help in the identification of pathogenic mechanisms involving mineral dusts. © 1997 Elsevier Science B.V.

Keywords: Biocells; ESCA; Fiberous asbestos; Surface chemical interaction

* Corresponding authors. Jacek Klinowski, tel.: (44-1223) 336514; fax: (44-1223) 336362; e-mail: jk18@cam.ac.uk. Terry L. Barr, tel.: (1-414)229 4085; fax (1-414)229 6958

PII S0304-3894(96)01850-X

1. Introduction

By virtue of its excellent thermal insulating, sound-proofing and tribological properties, asbestos was until relatively recently in widespread industrial use. Since it was established that human exposure to asbestos dusts may be harmful, a world-wide effort has been made to remove asbestos from the environment, although large amounts still remain in use [1].

Human exposure to certain mineral silicate dusts is often associated with the development of pneumoconiotic diseases. Silicosis, a fibrotic reaction of the lung, is induced by exposure to silica particles. Other particulate or fibrous silicates, such as asbestos and the zeolite erionite, can also induce fibrotic and cancerous lung diseases [2–4]. Of the silicate minerals, the amphiboles crocidolite and certain forms of anthophyllite, amosite asbestos and some other fibrous minerals, show pathogenic activity, evidently by processes which are related to their fibriform morphology [5–7]. Proposed toxic mechanisms have implicated iron in Fe-containing silicates which can catalyse and, in conjunction with phagocytic cells (neutrophils and macrophages), mediate the generation of free radicals and related reactive oxygen metabolites (ROM), such as superoxides, hydroxyl radicals and hydrogen peroxide [8,9].

Stanton's hypothesis, relating fibre dimension to the carcinogenicity of fibrous minerals, has been re-examined in the light of other evidence indicating a specific interconnection between an enhanced aspect ratio of some fibers and the activity of surface chemical interactions in the pathogenic process [10]. It has been suggested that properties such as the surface-charge zeta potential [11] and free radical generation from freshly fractured silica dust [12] contribute to particle cytotoxicity. Chemical modification by derivatizing the surfaces of fibrous silicates has revealed changes in reactivity in model in vitro cell toxicity studies, suggesting a multifactorial character of particle/cell interactions [13]. The adsorption of bovine serum albumin onto asbestos fibres has been shown by infrared spectroscopy and nuclear magnetic resonance (NMR) to be mediated by O–H–N hydrogen bonds [14].

Fig. 1. Structure of the amphiboles. (a) A (100) view (z-axis vertical) of the tetrahedral double-chain. T(1) is linked to three adjacent tetrahedra, T(2) to two. The chain extension is along z. The filled circles are OH groups bonded to 6-coordinate cations. (b) The metal sites in amphiboles shown in the same orientation as in (a). A ribbon of sub-regular metal-oxygen (MO_6) octahedra extends along z. OH groups are shown as filled circles, as in (a). There are three crystallographically distinct metal sites: M(1) is *cis*-bonded to two OH, M(3) is *trans*-bonded to two OH; M(2) is not bonded to OH. (010) mirror planes pass through M(3) sites and OH, doubling the number of M(1) and M(2) sites. The large circles are large 6–8 coordinate M(4) metal sites, forming either a highly distorted octahedron or a cubic antiprism. (c) A view of the structure looking down the z-axis (x-axis vertical, y-axis horizontal). This shows the characteristic chequer-board arrangement of the 'double-anvil' units in which each ribbon of octahedral metal sites is sandwiched between two facing tetrahedral double-chains. The large M(4) metals flanking the ribbon cross-link adjacent sandwiches. Where the double-chains are 'back-to-back' there is a large 'A site' which may be vacant or occupied by a large alkali metal cation (usually Na^+ or K^+). In cummingtonite the A site is vacant. Vertical straight lines are mirror planes, dotted lines outline the unit cell.

Attention has also been given to the role of iron in mediating toxic and carcinogenic processes [15]. Inhibition by the iron-chelate desferroxamine of asbestos-generated ROM formation suggests that the iron-catalyzed Fenton reaction is a critical mechanism in promoting free radical oxidative stress [16]. Generation of hydroxyl radicals seems to be related to the iron content at or near the surface of the mineral [17,18], which in certain forms of asbestos may be mobilized by endogenous chelators and reductants, such as

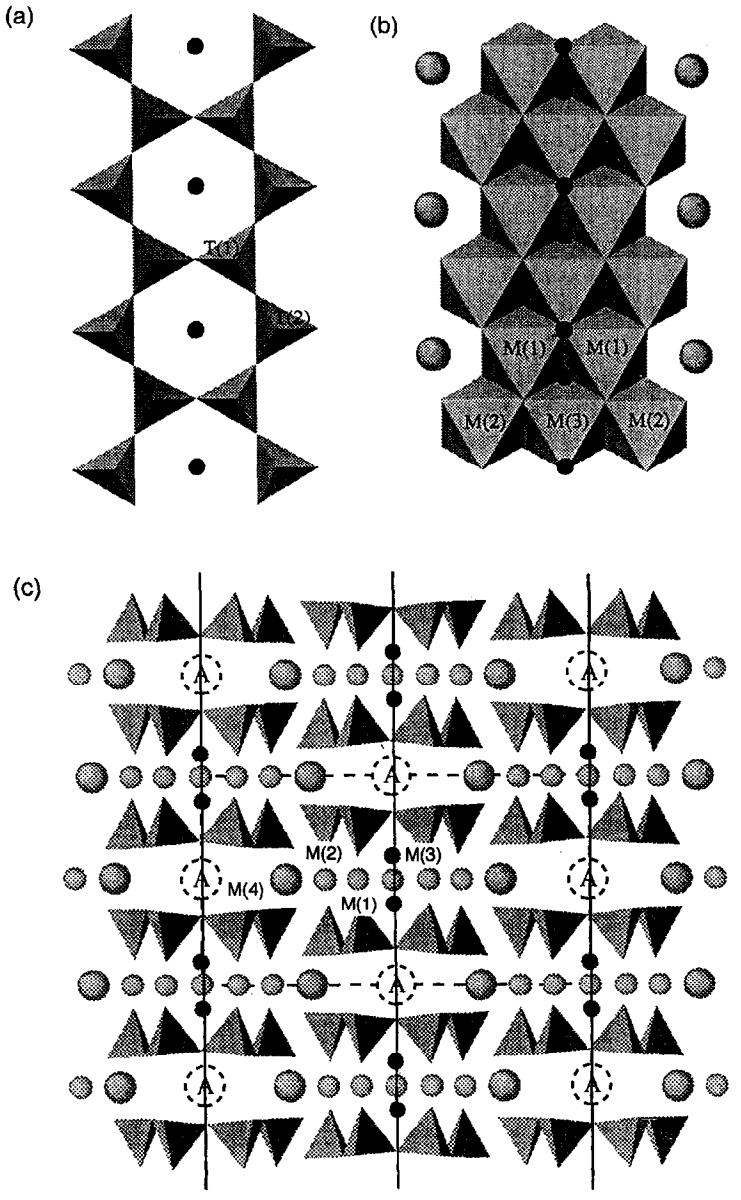

Table 1
Si(2p), Mg(2p) and O(1s) ESCA binding energies (in eV) in silica and several silicates

Materials	Si(2p)	Mg(2p)	O(1s)	Ideal Si/Mg ratio
Silica (SiO_2)	103.6	–	532.7	–
Anthophyllite	103.45	50.95	532.6	1.6
Talc	103.1	50.5	532.2	1.33
Montasite	102.5	50.0	532.0	1.2
Cummingtonite	102.2	50.25	531.55	1.15
Chrysotile	102.4	49.3	531.2	0.67
		50.1	532.3	

Error margin ± 0.1 eV.

citrate, ADP and ascorbic acid [19]. Iron-containing minerals can promote oxidative reactions with DNA in vitro [20]. The presence of iron-containing asbestos or ferruginous bodies in vivo may involve the deposition of adsorbed ferritin/hemosidirin molecules [21,22], although the contribution of the protein-bound iron to ROM production is unknown.

Sheet silicates known as the serpentines, particularly chrysotile and the fibrous forms of double-chain amphiboles, are the most commonly used type of asbestos [23–26]. As there seems to be a latency period of more than 20 years between exposure and the development of many pathological conditions, one may expect the harmful effects of asbestosis to be with us in the foreseeable future.

In recent years, the bulk chemical analysis of silicates has become the province of magic-angle-spinning (MAS) NMR [27]. The success of the technique prompted some researchers to question the need for the additional application of surface methods (to the depth of < 100 Å). However, recent work has established the importance of surface studies using high-resolution X-ray Photoelectron Spectroscopy (XPS), also known as ESCA (for Electron Spectroscopy for Chemical Analysis) [28]. Our ESCA studies of silicates and aluminosilicates [29,30], have rationalized the observed chemical shifts in terms of the relative differences in the covalency/ionicity of the Si–O and M–Al–O bonds (where M is the cation accompanying the aluminate subunit) [31] (Table 1, Fig. 1).

We have exposed asbestos to cellular systems under controlled conditions and then subjected both components of the mixture to ESCA surface analysis. We describe the changes in surface chemistry with respect to the relative concentration changes of Fe, Mg, Al and Si in the asbestos and the cells, and any indications of evolving chemical states.

2. Materials and methods

2.1. Materials

A bulk sample of asbestos was obtained from geological sources by Professor G. Mursky of the Geosciences Department of the University of Wisconsin-Milwaukee.

Except for crushing to a fine powder, no effort was made to dry, clean or otherwise modify it before the experiments. The question of the most appropriate preparation of the samples for ESCA analysis has been discussed previously [28]. Natural silicates are known to undergo various forms of mild surface degradation (surface-oriented non-crystallinity, deposition of adventitious carbon, formation of surface carbonyls and hydroxyls). We have found that these effects had only a very slight effect on the surface character of our samples.

2.2. Experimental protocol

For preliminary surface analysis by ESCA, a small quantity (ca. 100 mg) of asbestos was pressed into 6×4 mm wafers under 6500 psi pressure, suitable for ready insertion into the ESCA spectrometer. Samples used for cell culture studies were sterilized by autoclaving. Ehrlich cells, a murine tumor cell line, were used as the model cell culture system. Cells were grown to a confluent monolayer in a Petri dish in minimum essential medium (MEM) supplemented with 4% foetal bovine serum, and finally released by trypsinization. The cells were then transferred to another Petri dish and the silicate wafers added.

The four series of experiments involved: (1) incubated asbestos only (as crushed powder and wafers); (2) asbestos wafers immersed in culture medium; (3) asbestos wafers contacted with cells in culture medium, and (4) cells alone in culture medium. All samples were maintained for 7–9 days in a 5% CO_2, 95% air atmosphere in a Forma Scientific incubator at 37°C. The seeding density of cells was 3×10^4 cells ml^{-1} with silicate fibre mass concentration of 12.5 mg ml^{-1}. The cells and/or medium were detached from the silicate wafers by trypsinization, and the wafers were washed with distilled water (to destroy any attached cells), sedimented and centrifuged at 1600 g for 14 min. They were then washed again with distilled water and finally dried at 100°C. Wafers were visually inspected by light microscopy ($100 \times$) to ensure that no cell fragments remained on the surface. In a few cases the cell–silicate mixture was frozen on dry ice for 5–10 min and finally dried at a pressure of 10^{-9} torr in a Labconco freeze drier. The following samples were then subjected to ESCA analysis to establish the kind and amount of species present at or near the surface: (1) untreated asbestos; (2) asbestos following treatment without cells or medium; (3) asbestos separated following medium-only treatment; (4) asbestos following treatment with cells; (5) freeze-dried cells before adding to asbestos; (6) cells extracted from asbestos and then freeze-dried; and (7) freeze-dried asbestos–cell mixture.

2.3. Elemental analysis of cells

The iron and aluminium content of the Ehrlich cells was also measured before and after interaction with the silicate by Atomic Absorption Spectroscopy (AAS). Cells solubilized in 5% sodium dodecyl sulphate (SDS) were wet-digested using a 1:1 dilution with a hydrolysis solution of 50% $HClO_4$, 30% HNO_3 and 20% H_2O, followed by heating on a steam bath for 3 h. The resulting solutions were analyzed for iron by flame AAS using an IL model 357 AA/AE spectrophotometer. Standard solutions needed for

calibration, obtained from Fisher Scientific, were diluted to 0.5, 1.0 and 2.0 ppm, and all samples were analyzed simultaneously. The absorbance values were used to create a standard curve from which the concentrations were determined. We estimate the experimental errors in sample composition at $\pm 8\%$ of the absolute value. Cells solubilized in 1.0 ml of 5% sodium dodecyl sulphate (SDS) were also analyzed for cell protein content using a colorimetric Bio-Rad DC assay [32].

2.4. ESCA

ESCA studies were performed on a Hewlett-Packard (HP) 5950A spectrometer using a high-resolution X-ray monochromator, giving a binding energy scale specified by $Au(4f_{7/2}) = 83.98 \pm 0.05$ at a linewidth of < 1.0 eV. Some results were recorded on a Vacuum Generator (VG) ESCALAB system using a conventional Al–Ka anode. The background pressure during analysis in both instruments was ca. 1×10^{-9} torr. The charging shifts produced by the insulating samples were removed by using a binding energy scale established by a combination of electron flood gun adjustments and fixing the C(1s) binding energy of the hydrocarbon part of the adventitious carbon line at 284.6 eV [33]. We have used this well-established procedure in many studies of silicates [28,29].

3. Results

3.1. Asbestiform silicates

Asbestiform materials are derived from either sheet silicates or double-chain silicates known as the amphiboles. In sheet silicates two-dimensional octahedral (O) and tetrahedral (T) layers are variously linked via 'apical' oxygens to form T–O linkages. Depending on the composition and relative orientation of the layers, a variety of macroscopic structures, some of them fibrous, are generated [34]. Common sheet forms include the classic asbestos chrysotile [35].

The general formula of amphiboles, $W_{0-1}X_2Y_5Z_8O_{22}(OH,F)_2$, represents one-half of the atoms in a unit cell, where W stands for the 10–12 fold coordinate cations occupying the A structural sites (dotted circles in Fig. 2), X the 6–8 fold coordinate cations on M4 sites (in our sample Mg) (large circles), Y the 6-fold (octahedral) coordinate structural cations on M1, M2 and M3 sites, and Z refers to the 4-fold (tetrahedral) coordinate structural species in SI and SII sites. The occupancies of the various sites are controlled by the bonding chemistry, by size requirements and by the need to satisfy the local electric charge balance. Our sample was found to contain only Mg, Si, O and a small amount of Ca and Fe.

3.2. Structural characterization of the asbestos sample

The fibrous sample was originally designated as chrysotile, but we were aware that the precise identification of asbestiform silicates is rarely straightforward. Optical

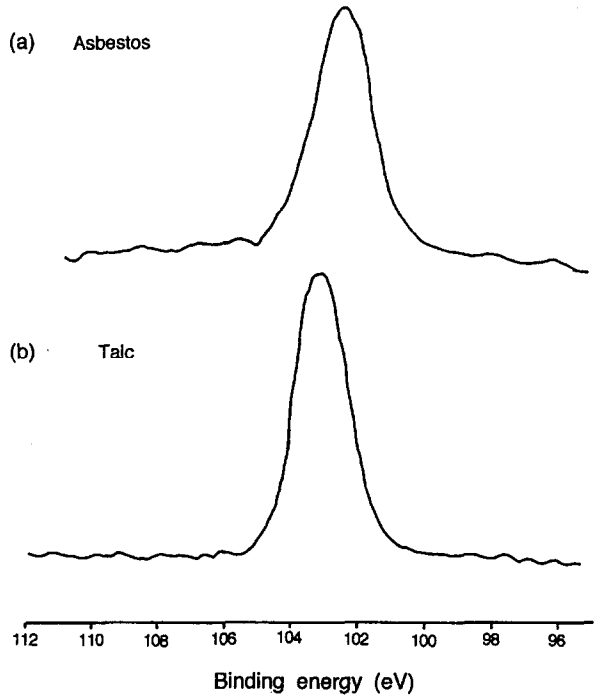

Fig. 2. Si(2p) ESCA spectra of: (a) asbestos, (b) talc.

microscopy confirms the fibrous character of our sample (not shown), while ESCA identifies it as a magnesiosilicate with Si/Mg = 1.2 ± 0.05. A small amount of Ca and Fe is also found, but other elemental species do not exceed trace quantities. The linewidths for the principal ESCA core level peaks indicate that the sample is monophasic. The Si(2p) and Mg(2p) binding energies for cummingtonite are similar to that measured, but the Si/Mg ratio of our sample is different from both chrysotile and cummingtonite and some binding energy shifts are to be expected (Fig. 2) [28,36]. X-ray diffraction also demonstrates that our sample is an amphibole of the cummingtonite class and not a sheet silicate. The identification of our sample as montasite, a magnesiosilicate with a fibrous asbestiform habit [34] is consistent with both the binding energy shifts for the cummingtonite class and with the unusual Si/Mg ratio.

3.3. Asbestos in biological media

ESCA shows the increase in the surface concentration of iron upon treatment of asbestos with the media and cells (Table 2). Typical 0–200 eV survey Fe(3p) ESCA spectra (Figs. 3 and 4b) show an increase in iron in asbestos contacted with the cells. After separation from the asbestos fibres, the concentration of Fe in the cells sharply increases. For as-received asbestos ESCA gives Si/Mg = 1.2. The ratio increases in asbestos contacted with cells, compared to that of the untreated material, indicating a

Table 2
Relative amounts of Si, Fe and Mg in asbestos before and after various treatments determined from the intensities of the appropriate lines in a 0–200 eV ESCA survey scan with respect to the intensity of the Si(2p) line taken as 30 units

Treatment	Fe(3p)	Mg(2p)	Si/Mg
As-received	2.2±0.18	9±0.56	1.2±0.12
A, M, I, W, D	⇑	8.75±0.70	1.3±0.10
A, M, C, I, W, D	⇑⇑	7.5±0.60	1.5±0.12

Error margin ±8% of the absolute value. Note that the ideal value of the Si/Mg ratio of cummingtonite is 1.15 (see text).
A = autoclaving; I = incubation; M = medium; C = cells; W = washing; D = drying; ⇑ = increase; ⇑⇑ = strong increase.

decrease in Mg concentration. This is opposite to the behaviour observed for the cell-treated amphibole cummingtonite. No aluminium was detected in the cells after interaction with asbestos.

Fig. 5 shows a typical C(1s) spectrum of asbestos subjected to various treatments. In cell-treated asbestos we find large amounts of N–C=O, C–N and C–O bonds, suggesting that cells or their fragments cling to the surface of the silicate even after careful washing. This enhanced presence of carbonaceous materials is not found in the C(1s) spectra (Fig. 5a,b) of untreated and media-treated asbestos. We also find an increase in the O(1s), Si(2p) and Mg(2p) binding energies (see Table 3) as asbestos is subjected to the medium and the cells. The increase in the Si(2p) binding energy suggests an increase in Si content in the cell-treated asbestos, indicating that the silicate acts as a positive ionic site under the influence of cells and Si–O bonds. Table 4 shows the presence in cell-treated asbestos of additional elements such as P, Na, Al and N. The presence of the significant N(1s) at ca. 399.8 eV and the character and positions of the C(1s) peaks, strongly suggest the retention on the surface of the silicates of significant depositions of organic units. The presence of phosphorus and the C(1s) binding energies suggest the presence of substantial medium residue, along with cellular species. Once again, a key feature is the obvious presence of substantial amounts of C–O–C*=O at ca. 288.8 eV [37].

Cells contacted with the media and asbestos contacted only with the media were examined by atomic absorption to determine changes in elemental content. Fig. 6 shows a six-fold increase in iron content in asbestos-treated cells compared with cells before silicate treatment. To obtain the true iron content of the cells and cells contacted with asbestos, protein analysis was done by Bio-Rad protein assay. The results reveal a seven-fold increase in iron content in treated cells (ca. 35 mg Fe/mg of cell protein) compared with that for the cells only (0.05 mg Fe/mg of cell protein). It appears that the iron has been extracted from the silicate, transported through the media and taken up by the cells via an ion-exchange process. We observe an increase in both Fe^{2+} and Fe^{3+} compared to the as-received asbestos. In the presence of cells iron apparently segregates migrates from the bulk towards the surface of the silicate. ESCA results for the untreated material do not show nearly as much iron as the material which has been in contact with the cells, thus supporting the concept of a bulk-to-surface segregation. Note that our

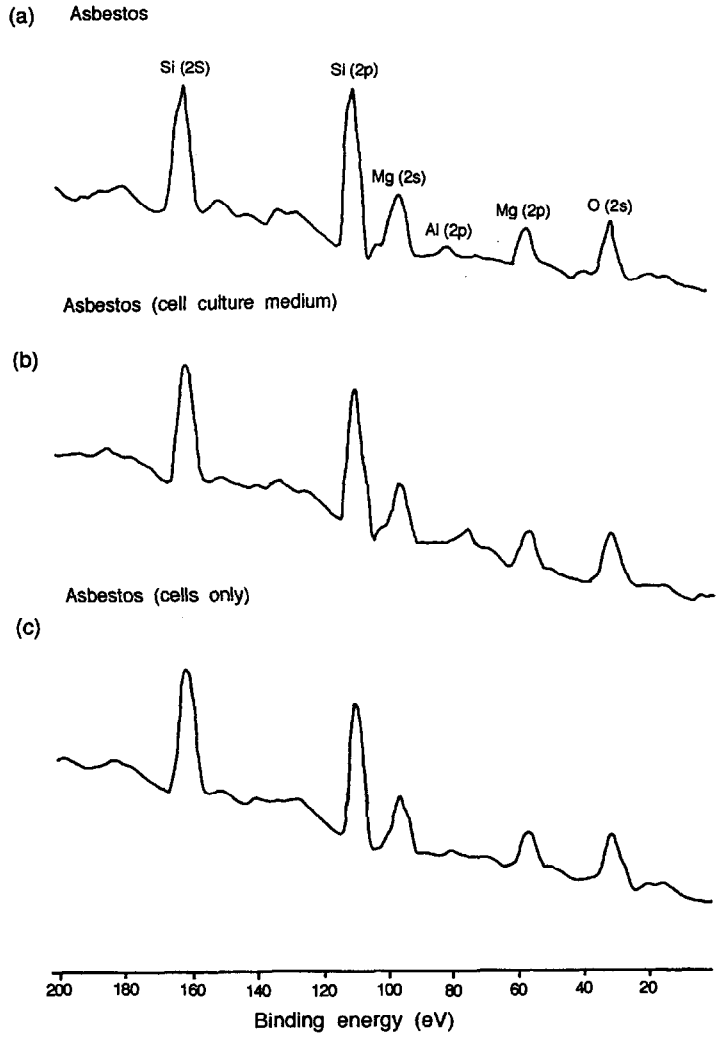

Fig. 3. 0–200 eV ESCA survey spectra of asbestos: (a) untreated, (b) treated in cell culture medium, and (c) contacted with cells.

results suggesting the possible extraction of Fe from our silicate do not contradict the conclusion of Deer et al. [34] regarding the extra-lattice origins of most Fe.

The cell culture medium, composed of MEM and bovine serum (which contains iron necessary for cell growth) is a possible source of the extra iron found in the cells after contact with asbestos. In order to establish the origin of the extra Fe, we have monitored the iron content of the cell culture medium in two independent experiments, after 6 and 9 days incubation. We found that the Fe content of the medium contacted with the silicate (0.65 μg Fe) differed from the control not involving contact with the silicate

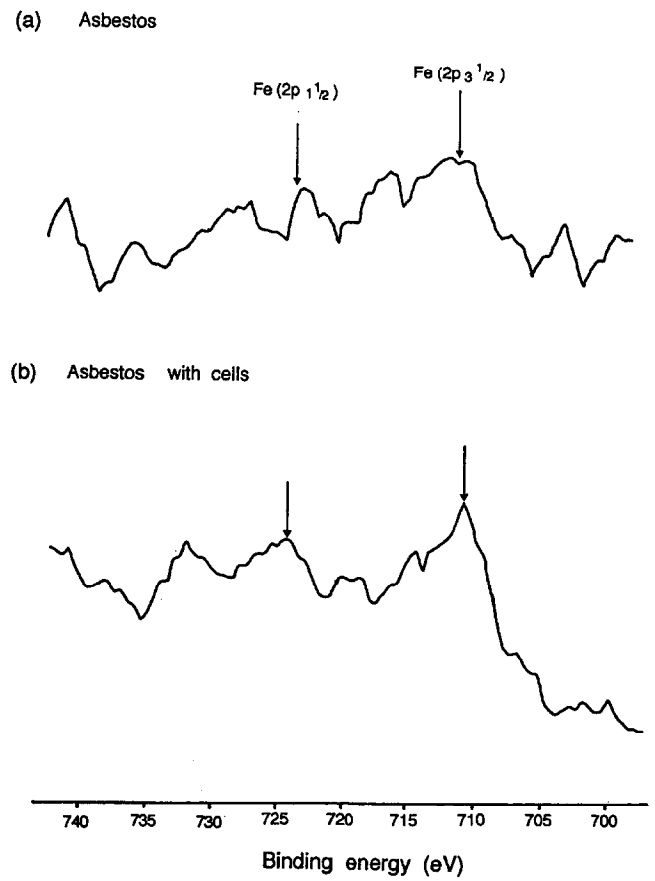

Fig. 4. Fe(3p) ESCA spectra of asbestos: (a) untreated, (b) contacted with cells.

(0.642 μg Fe) by only ca. $\pm 1\%$, which indicates that the iron uptake by the cells is triggered by the silicate.

3.4. Freeze-dried cell–asbestos mixture

We have used ESCA to study samples of freeze-dried cells contacted with asbestos, where the cells were grown on the surface of the silicate wafer under controlled conditions and the sample was subsequently freeze-dried. Na, Al, Si, Fe, Mg and P were found on the surface. During the analysis of the top and bottom parts of the pre-freeze-dried suspension, more cells and less silicate were detected on the top, but a substantial amount of both species was found on both sides of the freeze-dried mixture. Detailed analysis of the Si(2p) ESCA spectra revealed evidence for the presence of three different states of silicon (Fig. 7). One of these appears to be that from 'clean chrysotile', but the other two yield binding energies which indicate chemical involvement with the cells themselves, possibly through the formation of C–O–Si and C–Si bonds. A multifaceted

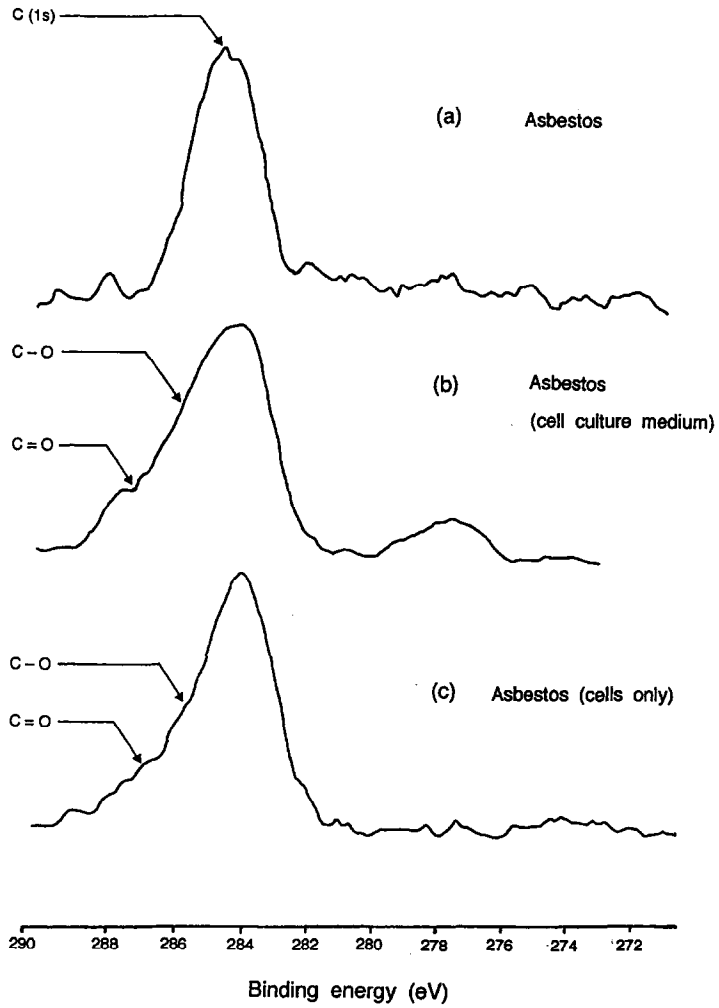

Fig. 5. C(1s) ESCA spectra of asbestos: (a) untreated, (b) treated in cell culture medium, and (c) contacted with cells.

Table 3
ESCA binding energies referenced to C(1s) = 284.6 eV of the elemental components of asbestos before and after various treatments

ESCA peak	Binding energy (eV)		
	As-received asbestos	Asbestos in medium	Asbestos in medium with cells
O(1s)	532.0	532.0	532.15
Si(2p)	102.5	102.6	102.7
Mg(2p)	50.0	50.0	50.7

Error margin ±0.1 eV. Note the large upward shift in the Mg(2p) binding energy after contacting asbestos with the cells.

Table 4
Trace element content of asbestos (determined by ESCA) before and after various treatments

Element	Asbestos alone	Asbestos in medium	Asbestos in medium and cells
Nitrogen	S	MS	M
Iron	MS	M	ML
Aluminum	MS	MS	MS
Sodium	MS	MS	MS
Phosphorus	ML	MS	MS

S = small; M = medium; L = large; MS = medium small; ML = medium large.

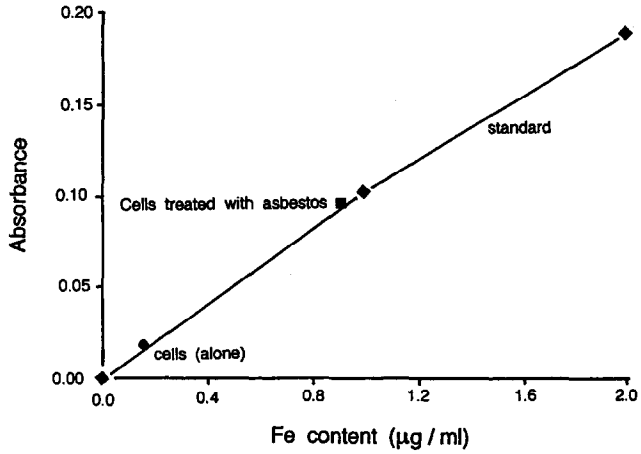

Fig. 6. Iron content of cells before and after contact with asbestos.

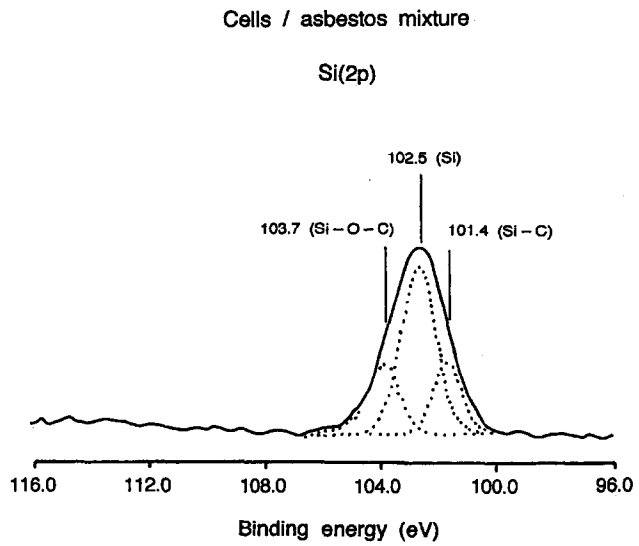

Fig. 7. Si(2p) ESCA spectra of freeze-dried cell-asbestos mixture.

structure of this kind is not unknown when a silicate system is interfaced with another material under conditions of substantial physical strain. We can also discern some of the surface characteristics of frozen cells, as well as surface-retained components of the medium. The C(1s) spectra (Fig. 8) suggest the presence of: (i) N–C = O (BE_C = 287.7 eV), (ii) C–O–C (BE_C = 285.8 eV), (iii) C–H (BE_C = 284.6 eV), (iv) C = N (BE_C = 286.1 eV), (v) C–OH (BE_C = 286.8 eV) (where BE_C denotes the C(1s) binding energy). Very similar results were obtained for the Si(2p) and C(1s) spectra of freeze-dried cells exposed to the amphibole cummingtonite [36].

3.5. Surface chemistry of cells with and without contact with asbestos

The ESCA spectra of asbestos treated only with the medium and then subjected to the remaining processing steps [36] are very similar to those of untreated asbestos, particularly with respect to the relative concentration of the lattice cations. Close examination reveals that, despite their presence in the medium, very little NaCl or $NaHCO_3$ is adsorbed onto the surface. Given that soluble salts should be removed during washing, this is hardly surprising. On the other hand, the less soluble organics (glucose and amino acids such as *l*-glutamine) may not be entirely washed away. Also, hemoglobin, sugars and cholesterol, the main components of blood, may be adsorbed from the serum, along with triglycerides and phospholipids. However, the latter should give rise to a distinct $P(2p_{3/2})$ ESCA peak, while only a moderate amount of P is actually detected. In order to determine the composition of the residue left upon contact with the medium, we refer

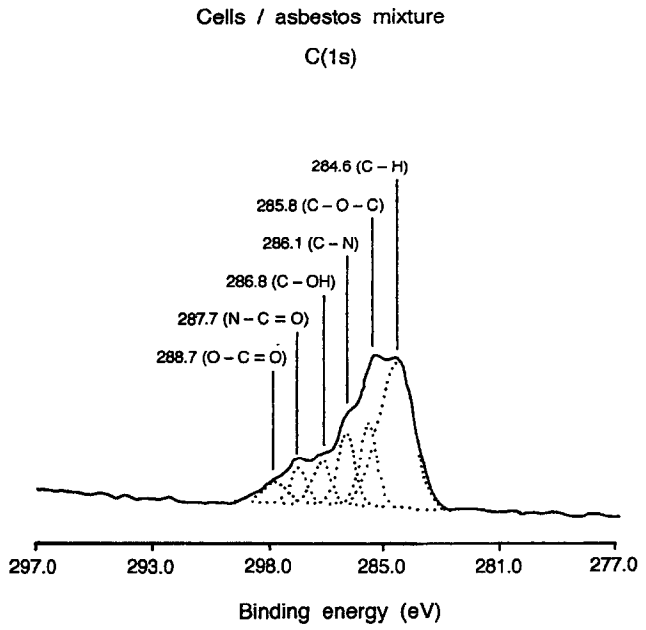

Fig. 8. C(1s) ESCA spectra of freeze-dried cell-asbestos mixture.

Table 5
Binding energies and (in brackets) linewidths (both in eV) of elemental peaks in the ESCA spectra of freeze-dried cells

	Treatment of cells	
	Untreated	After contact with asbestos
C(1s)	284.6 (1.67)	284.6 (1.68)
	286.0	286.0
	287.7	287.7
O(1s)	531.7 (3.0)	531.4 (3.0)
	531.2	530.2
	532.6	532.4
	533.2	533.0
$P(2p_{3/2})$	133.2 (1.8)	132.9 (1.85)
N(1s)	399.7 (1.8)	399.5 (1.95)
	401.5 medium	401.3 small
	402.7 (1.8)	402.4
Na(1s)	1071.2	1071.3
$Ca(2p_{3/2})$	Medium	Very small
Si(2p)	0	Small
Al(2p)	0	0
$Fe(2p_{3/2})$	0	0
Mg(2p)	0	Very small

'Medium', 'small' and 'very small' refer to spectral intensities. When such qualification is absent, intensity is high.

to our earlier results and to those of Beamson and Briggs [37]. The C(1s) spectrum described in Tables 5 and 6 indicates the presence of C–N–H, C–O–H, C*–O–C = O and NH–C = O species on the surface of the asbestos. This is consistent with the adsorption of a mixture of glutamine, glucose, cholesterol and triglycerides.

Table 6
Elemental concentration ratios (as determined by ESCA) in asbestos and cells after various treatments

	N/C	O/Si	N/O	P/N	P/O	C/Si	O/C
Untreated cells	0.1	–	0.5	0.236	0.118	–	0.2
Cells after contact with asbestos	0.085	–	0.68	0.255	0.17	–	0.13
Mixture of cells and asbestos	0.24	3.6	0.14	0	0	2.16	1.7
Asbestos after separation from cells	0.15	3.4	0.09	0	0	2.05	1.8
	0.13	3.7	0.094	0	0	2.6	1.4

The solid obtained from freeze-drying cells not contacted with asbestos (Table 5) is expected to contain only cells, as the medium in which the cells were suspended should have been dissipated upon freeze-drying [38]. In separate experiments, the cells were: (i) freeze-dried and examined, and (ii) separated from the asbestos and freeze-dried. The relative surface composition of the samples is given in Table 6. The binding energies of the cellular O, P and N are reduced (Table 5), making the cells more negative during the

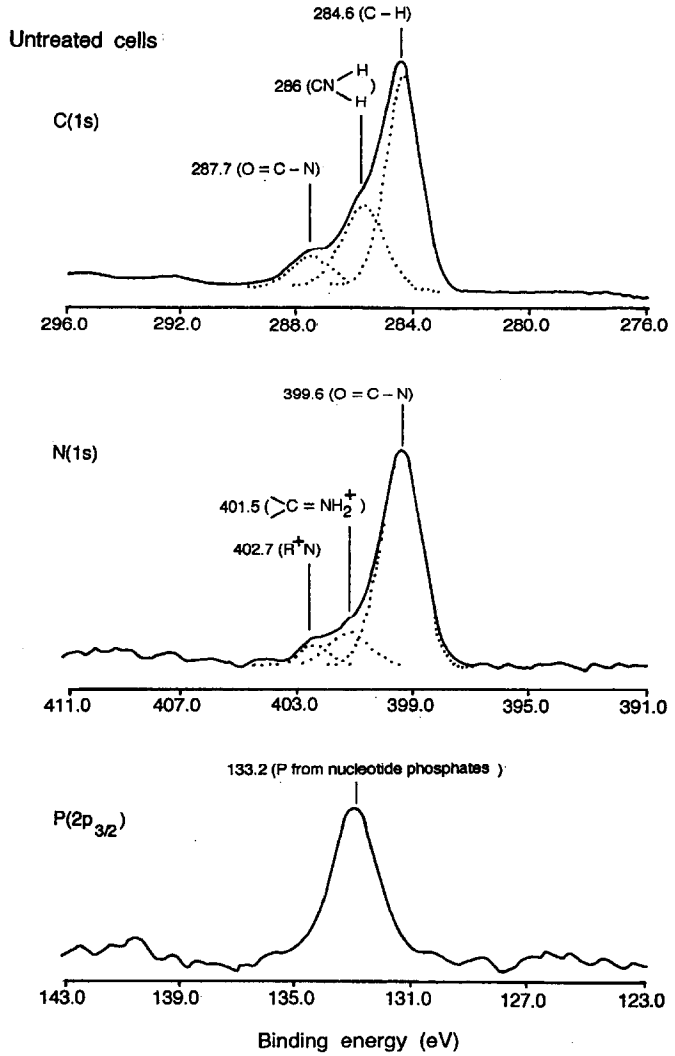

Fig. 9. (a) C(1s), (b) N(1s), and (c) P(2p) ESCA spectra of untreated freeze-dried cells. Note the complex peak structure of the C(1s) and N(1s) spectra.

treatment with the asbestos (see above). The advantage over the medium-only system is that no O(1s) peak from asbestos and no cations are present. Surprisingly, the N/C ratios for the cell-only samples are smaller than for the cell-coated asbestos, but the N/O ratio is higher and so is the phosphorus content (Table 6, Fig. 9). The C(1s), O(1s) and N(1s) binding energies show the presence of C_xH_y, C–NH and O = C–NH groupings (Fig. 9a). This does not exclude the presence of C–OH species, but substantial amounts of them are not found. In addition, there is clear evidence for the presence of organic phosphate (Fig. 9c). All this indicates the detection of cells following the removal of the water and lipids. The main species detected are proteins with some nucleic acids with their interconnecting phosphate bridges. The reason for the absence of the O–C*–OR units of the lipid and the C*–OH species of the polysaccharides is not clear, unless they have also been selectively washed away.

Before we attribute the latter results to the presence of cells, we note that the surface of freeze-dried cells may be coated by the medium. However, the differences between the spectra of the cells and the medium suggest that the surface of the freeze-dried cells is at least partially available to ESCA detection. The C, N, P, Si and O ESCA results for the freeze-dried asbestos–cell mixture (Figs. 7 and 8) confirm the presence of organic species and other components of the suspension, with the structure of the C(1s) manifolds and the N/C ratios similar to that when the medium adheres to the surface of cummingtonite. However, the presence of phosphorus and the binding energies measured in the cummingtonite experiment indicate the detection of species of cellular rather than of medium origin. ESCA is clearly detecting protein units [37], but their origin is unclear.

4. Conclusions

This work is a continuation of our efforts to characterize the chemistry of interaction of living cells with surfaces of silicate minerals. In the course of the programme we have used primarily ESCA, but also microscopic and XRD studies as well as atomic absorption spectroscopy measurements of cell-containing suspensions. ESCA is particularly suitable to this kind of work, because it alone permits simultaneous monitoring of the outermost surfaces of the cells and the silicates before, during and after their interaction. This paper is concerned with the growth of murine tumor cells with montasite, a rarely studied amphibole asbestos. The results show that the cells retain most of their ESCA signature (the amount and kind of carbon, nitrogen and phosphorous containing species) after removal from the silicate and freeze drying, and that there is a thin, optically undetectable, layer of cells on the silicate after completion of conventional biological separation procedures. On the other hand, the asbestos is found to be chemically altered by the growing cells. The primary alteration is the appearance on the surface of montasite of significant amounts of Si–O–C and Si–C bonds, suggesting the formation of chemical 'bridges' between the growing cells and the asbestos. Mg and Fe are extracted from the cells into the silicate and possible mechanisms of this process are suggested. While this is outside the scope of this work, it is intriguing to speculate about possible links between these observations.

Acknowledgements

We are grateful to the referees for their comments, which we have found most useful.

References

[1] V. Timbrell, Characteristics of the international union against cancer standard reference sample of asbestos, in H.A. Shapiro (Ed.), Proc. Intern. Conf. on Pneumoconiosis, Oxford, U.K., 1970, pp. 28–36.
[2] R.C. Brown, P. Carthes, J.A. Hoskins, E. Sara and C.F. Simpson, Surface modification can affect the carcenogenicity of asbestos, Carcinogenesis 11 (1990) 1883–1885.
[3] K.R. Spurney, Natural fibrous zeolites and their carcinogenicity — a review, Sci. Total Environ., 30 (1983) 147–166.
[4] B.T. Mossman, Mechanisms of asbestos carcinogenesis and toxicity: The amphibole hypothesis revisited, Br. J. Industr. Med., 50 (1993) 673–676.
[5] M.F. Stanton, M. Layard, A. Tegeris, E. Miller, M. May, E. Morgan and A. Smith, Relation of particle dimension to carcinogenicity in amphibole asbestoses and other fibrous minerals, J. Nat. Cancer Inst., 67 (1981) 965–975.
[6] J.G. Herring and W. Stumn, Oxidative and reductive dissolution of minerals, in Mineral–Water Interface Geochemistry (M.F. Hochella, Jr. and A.F. White), Reviews in Mineralogy, 123 (1990) Chap. 11.
[7] C.C. Addison, W.W. Addison, G.H. Weal and J.H. Sharp, Amphiboles, Part I, The oxidation of crocidolite, J. Chem. Soc. (1982) 1768–1771.
[8] T. Ishizaki, E. Yano and P.H. Evans, Crocidolite induces reactive oxygen metabolites generation from human polymorphonuclear leukocytes, Environ. Res., 66 (1994) 208–216.
[9] D.W. Kamp, P. Graceffa, W.A. Pryor and S.A. Wietzman, The role of free radicals in asbestos-induced diseases, Free Rad. Biol. Med., 12 (1992) 293–315.
[10] J. Dunnigan, Biological effects of fibers: Stanton's hypothesis revisited, Environ. Health Perspect. 57 (1984) 333–337.
[11] W.G. Light and E.T. Wei, Surface charge and hemolytic activity of asbestos, Environ. Res., 13 (1977) 135–145.
[12] V. Vallyathan, X. Shi, N.S. Dalal, W. Irr and V. Castranova, Generation of free radicals from freshly fractured silica dust, Am. Rev. Resp. Dis., 138 (1988) 1213–1219.
[13] P.H. Evans, R.C. Brawn and A. Poole, Modification of the in vitro activities of amosite asbestos by surface derivatization, J. Toxicol. Environ. Health, 11 (1983) 535–543.
[14] R. Dumitru-Stanescu, C. Mandravel and C. Bercu, Infrared and nuclear magnetic resonance studies on some properties of asbestos–albumin interactions, Analyst 119 (1994) 689–691.
[15] S.H. Kon, Biological autoxidation, Part 1, Decontrolled iron: An ultimate carcinogen and toxicant: An hypothesis, Med. Hypoth., 4 (1978) 445–471.
[16] S.A. Weitzman and P. Graceffa, Asbestos catalyzes hydroxyl and superoxide generation from hydrogen peroxide, Arch. Biochem. Biophys., 228 (1984) 373–376.
[17] A.J. Ghio, J. Zhang and C.A. Piantadosi, Generation of hydroxyl radical by crocidolite asbestos is proportional to surface [Fe^{3+}], Arch. Biochem. Biophys., 298 (1992) 646–650.
[18] D.M. Miller, G.R. Buettner and S.D. Aust, Transition metals as catalysts of autooxidation reactions, Free Rad. Biol. Med., 8 (1990) 95–108.
[19] L.G. Lund and A.E. Aust, Iron mobilization from asbestos by chelators and ascorbic acid, Arch. Biochem. Biophys., 278 (1990) 60–64.
[20] M. Berger, M. De Hazen, A. Nejjari, J. Fournier, J. Guignard and H. Pezerat, Radical oxidation reactions of the purine moiety of 2′-deoxyribonucliosides and DNA by iron-containing minerals, Carcinogenesis 14 (1993) 41–46.
[21] F.D. Pooley, Asbestos bodies, their formation, composition and character, Environ. Res., 5 (1972) 363–379.
[22] F.D. Pooley, Mineralogy of asbestos: The physical and chemical properties of the dusts, Semin. Oncol., 8 (1981) 243–249.

[23] J.S. Harrington, Chemical studies of asbestos, Ann. NY Acad. Sci., 132 (1965) 31–47.
[24] J.K. Dewaale and F.C. Adams, The surface characterization of modified chrysotile asbestos, Scanning Electron Microscopy 2 (1988) 209–228.
[25] A.A. Hodgson, Asbestos, John Wiley, New York, 1979, Vol. 1, pp. 67–114.
[26] J. Zussman, The crystal structures of amphibole and serpentine materials, 1978, National Bureau of Standards Special Publication No. 506.
[27] G. Engelhardt and D. Michel, High-resolution Solid-State NMR of Silicates and Zeolites, John Wiley, Chichester, 1987.
[28] T.L. Barr, Modern ESCA: The Principles and Practice of X-Ray Photoelectron Spectroscopy, CRC Press, Boca Raton, Chap. 8, 1994.
[29] T.L. Barr, An ESCA study of Si as it occurs in adsorbents, catalysts and thin films, Appl. Surface Science 15 (1983) 1–35.
[30] T.L. Barr, The nature of the relative bonding chemistry in zeolites: An ESCA study, Zeolites 10 (1990) 760–765.
[31] D.W. Breck, Zeolite Molecular Sieves: Structure, Chemistry and Use, John Wiley, London, 1974.
[32] O.H. Lowry, N.J. Rosebrough, A.L. Farr and R.J. Randell, Protein measurement with the folin phenol reagent, J. Biol. Chem., 193 (1951) 265–275.
[33] T.L. Barr and S. Seal, Nature of the use of the adventitious carbon as a binding energy standard, J. Vac. Sci. Technol., A13 (1995) 1239–1246.
[34] W.A. Deer, R.A. Howie and J. Zussman, An Introduction to Rock Forming Minerals, 2nd Ed., Longman, London, 1992, pp. 223–230, 279 and 324–344.
[35] B. Velde, Introduction to Clay Minerals, Chapman and Hall, London, 1992, pp. 60–61.
[36] S. Seal, S. Krezoski, S.E. Hardcastle, T.L. Barr, D.H. Petering, C.-F. Cheng, J. Klinowski and P.H. Evans, Investigations of the surface chemistry of pathogenic silicates, J. Vacuum Sci. Technol., A13 (1995) 1261–1266.
[37] G. Beamson and D. Briggs, High Resolution XPS of Organic Polymers, John Wiley, Chichester, UK, 1992.
[38] R.I. Freshney, Culture of Animal Cells, 2nd Ed., Viley-Liss, New York, 1987.